



Nucleon PDF separation with the collider and fixed-target data

Sergey Alekhin

Institute for High Energy Physics, Nauki 1, Protvino, Moscow region, 142281 Russia

Johannes Blümlein, Kristin Lohwasser

Deutsches Elektronensynchrotron DESY, Platanenallee 6, D–15738 Zeuthen, Germany

Lea Michaela Caminada

Physik Institut, Universität Zürich, Winterthurerstraße 190, CH–8057 Zürich, Switzerland

Katerina Lipka, Ringaile Plačakytė

Deutsches Elektronensynchrotron DESY, Notkestraße 85, D–22607 Hamburg, Germany

Sven-Olaf Moch

II. Institut für Theoretische Physik Universität Hamburg, Luruper Chaussee 149, D-22761 Hamburg, Germany

Roberto Petti

Department of Physics and Astronomy, University of South Carolina 712 Main Street, Columbia, SC 29208, USA

Abstract

We consider the impact of the recent data obtained by the LHC, Tevatron, and fixed-target experiments on the nucleon quark distributions with a particular focus on disentangling different quark species. An improved determination of the poorly known strange sea distribution is obtained due to including data from the neutrino-induced deep-inelastic scattering experiments NOMAD and CHORUS. The impact of the associated ($W + c$) production data by CMS and ATLAS on the strange sea determination is also studied and a comparison with earlier results based on the collider data is discussed. Finally, the recent LHC and Tevatron data on the charged lepton asymmetry are compared to the NNLO ABM predictions and the potential of this input in improving the non-strange sea distributions is evaluated.

Keywords: Parton distributions, strangeness, hadron colliders

1. Introduction

The nucleon quark distributions are important ingredients of the high-energy hadron collision phenomenology, particularly at large Bjorken x , since these are the quarks, which dominate the partonic content of the nucleon for these kinematics. The fixed-target inclusive deep-inelastic scattering (DIS) data, which play a central role in the determination of the parton distribution

functions (PDFs), provide a constraint only on the linear combinations of the quark distribution. Therefore, the global PDF fits are commonly based on a combination of the DIS data with ones for the Drell-Yan (DY) process, which yield a supplementary constraint on the PDFs. At that the strange sea distribution can be independently determined from the data on the c -quark production in neutrino-nucleon DIS probing the strange sea by the charged-current transition $s \rightarrow c$. If the

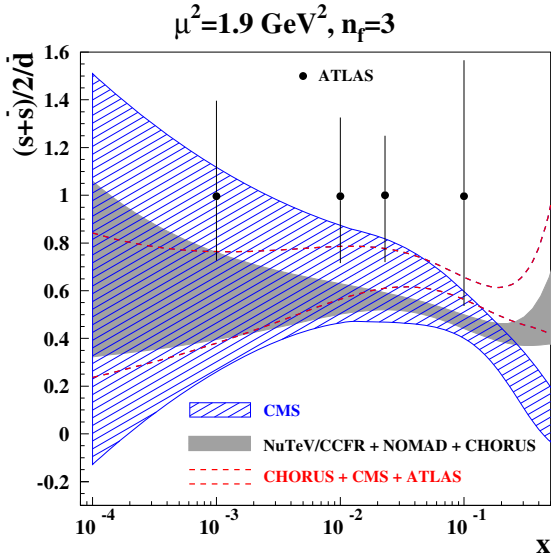


Figure 1: The 1σ band for the strange sea suppression factor $r_s = (s + \bar{s})/2/\bar{d}$ as a function of the Bjorken x obtained in the variant of the present analysis based on a combination of the data by NuTeV/CCFR [1], NOMAD [2], and CHORUS [3] (shaded area) in comparison with the results obtained by CMS [10] (hatched area), in the ATLAS $epWZ$ -fit [9, 14] (circles), and with the variant of present analysis based on combination of the data by CHORUS [3], CMS [8], and ATLAS [9] (dashes) at different values of x . All quantities refer to the factorization scale $\mu^2 = 1.9 \text{ GeV}^2$.

c -quark produced is detected by its semi-leptonic decay into a muon, this process can be triggered by two muons in the final states. This signature was used by the NuTeV/CCFR experiments [1] at Tevatron and the NOMAD experiment [2] at CERN. Alternatively, the events with a c -quark in the final state can be selected by the hadronic decays of charmed hadrons using the emulsion technique, like in the CHORUS experiment [3]. The NuTeV/CCFR data [1] have been employed to constrain the strange sea in the ABM PDF fit [4, 5, 6]. In the present proceedings we describe how the recent NOMAD [2] and CHORUS [3] data can further improve the strange sea determination. We also discuss the associated $(W + c)$ production in the proton-proton collisions measured by the CMS [8] and ATLAS [9] experiments at the LHC. Similarly to the case of neutrino-induced DIS, this process receives essential contributions from the charged-current transition $s \rightarrow c$. Therefore, it can be also used to pin down the strangeness contribution to the nucleon. Finally, we check the recent data on the charged lepton asymmetry A_l by the CMS [10] and DO [11] experiments measured in (anti)-proton-proton

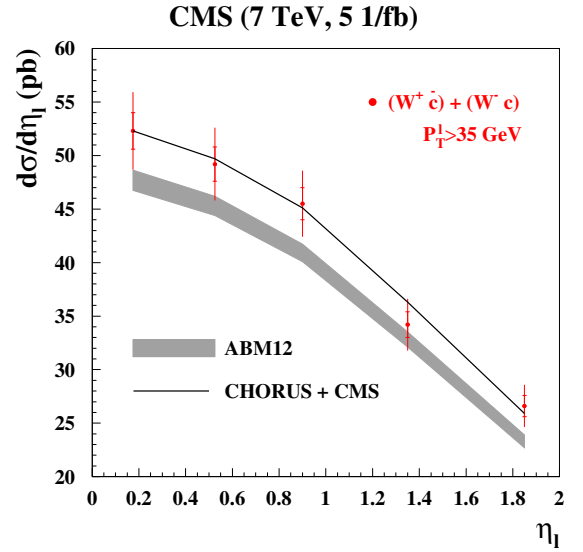


Figure 2: The CMS data on $(W + c)$ production [8] in comparison with the ABM12 predictions (shaded area) and the variant of ABM12 fit [6] with only the CHORUS charm [3] and the CMS $(W + c)$ data used to constrain the strange sea.

collisions w.r.t. the ABM12 PDFs [6]. Since the A_l measurement gives a constraint allowing to separate the u - and d -quark distributions this comparison demonstrates a further trend in determination of the non-strange quark PDFs.

2. Strange sea improvement

The NOMAD experiment collected about 15K dimuon events in the neutrino-nucleon DIS [2] exceeding the total statistics of earlier NuTeV/CCFR samples [1] by a factor of 1.5. Furthermore the NOMAD beam energy is essentially lower than the NuTeV/CCFR one that allows to probe the strange sea in the kinematic region inaccessible for NuTeV/CCFR, up to $x \sim 0.5$. The strange sea distribution can be extracted from the dimuon data provided the semi-leptonic branching ratio of the produced charmed hadrons is known. Meanwhile, their production rate essentially depends on the beam energy E_ν therefore an effective semi-leptonic branching ratio $B_\mu(E_\nu) = \sum_h r_h(E_\nu) B_\mu^h$ where $r_h(E_\nu)$ is the relative production rate of hadron h and B_μ^h is its semi-leptonic branching ratio, also depends on E_ν . We take into account this dependence employing an empirical parameterization of Ref. [2]

$$B_\mu(E_\nu) = \frac{B_\mu^{(0)}}{1 + B_\mu^{(1)}/E_\nu} \quad (1)$$

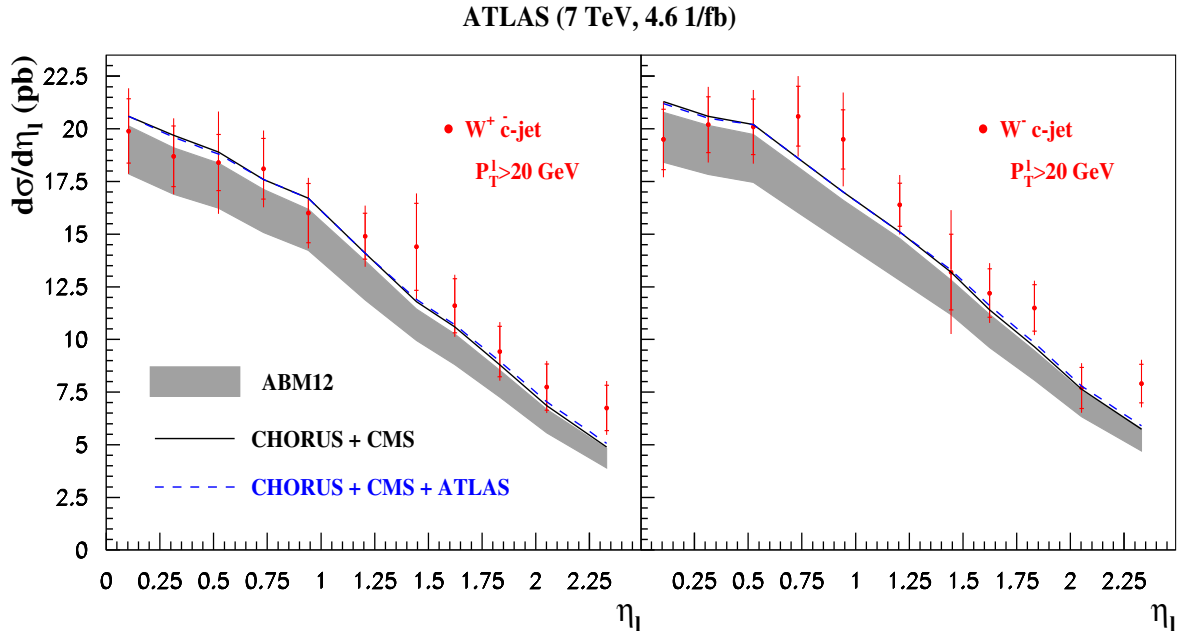


Figure 3: The same as in Fig. 2 for the ATLAS ($W^+ + \bar{c}$) (left) and ($W^- + c$) (right) data [9]. The variant of the ABM12 fit [6] with only CHORUS charm data [3] in combination with the CMS and ATLAS ($W + c$) ones [8, 9] used to constrain the strange sea is displayed by dashes.

with the parameters $B_\mu^{(0,1)}$ constrained by the existing data on B_μ [12, 13]. The values of $B_\mu^{(0)} = 0.0933(25)$ and $B_\mu^{(1)} = 5.6 \pm 1.1$ obtained in the present analysis are in agreement with the ones obtained by NOMAD [2]. With these values the parameterization Eq. (1) flattens in the beam energy range of NuTeV/CCFR and is consistent with the value of B_μ used in the earlier ABM12 fit [6].

The CHORUS experiment collected 2013 events with the charmed hadrons produced in the neutrino-nucleon DIS using the emulsion detection technique [3]. This is much smaller than the statistics of the dimuon experiments. However, due to the charm-decay vertex reconstruction, the CHORUS data are not sensitive to the corresponding branching ratios and provide in this way a complementary constraint on the strange sea.

The strange sea distribution obtained in the updated version of the ABM12 fit where the NOMAD and CHORUS data included is given in Fig. 1 as a ratio $r_s = (s + \bar{s})/2\bar{d}$ quantifying the suppression of the strange sea w.r.t. the non-strange one. It is roughly constant in a wide range of x and consistent with the value obtained earlier in our analysis of the NuTeV/CCFR dimuon data. However, the error in the updated determination of the strange sea at $x \gtrsim 0.01$ is improved up to a factor 2, mainly due to the impact of the NOMAD data [2] (cf.

more details in Ref. [7]). The CHORUS data [3] somewhat overshoot the fit and therefore pull the strange sea up.

The same is valid for the CMS and ATLAS data on ($W + c$) production [8, 9], cf. Figs. 2, 3, although in this case the tension can be at least partially explained by the impact of the still missing NNLO QCD corrections to this process. Note, the ATLAS data are in a good agreement with the predictions based on a variant of the ABM12 fit with only CHORUS and CMS data are used to constrain the strange sea, while the CMS ones are also described very well in this variant of fit. This demonstrates a good agreement between these three samples, which all together prefer enhanced strange sea. To check the upper margin of r_s allowed by this data subset we consider the variant of the fit with the NuTeV/CCFR and NOMAD data dropped and only the CHORUS, CMS, and ATLAS data used to constrain the strange sea. In this case the value of r_s at $x \sim 0.1$ is enhanced as compared to the determination based on the combination of the NuTeV/CCFR, NOMAD, and CHORUS data. However the difference is within 2σ and it does not exceed 20% at maximum.

At the same time, the strange sea obtained in the ATLAS PDF analysis [14] is comparable with the non-strange one, cf. Fig. 1. The analysis of Ref. [14] is

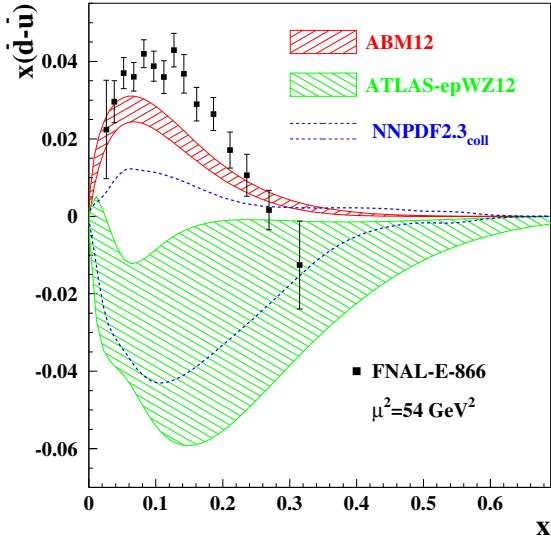


Figure 4: The 1σ band for the iso-spin asymmetry of the sea $x(\bar{d} - \bar{u})$ at the scale of $\mu^2 = 54 \text{ GeV}^2$ as a function of the Bjorken x obtained in the ABM12 fit [6] (right-tilted hatch) in comparison with the corresponding ones obtained in the ATLAS [14] (left-tilted hatch) and the NNPDF [16] (dashes) analyses using only the LHC and HERA collider data. The values of $x(\bar{d} - \bar{u})$ extracted from the FNAL-E-866 data [15] within the Born approximation are displayed as full circles.

based on the ATLAS data on the inclusive production of the W - and Z -bosons taken in combination with the HERA inclusive DIS data, while all fixed-target DIS and DY data are not considered. However, the result of the ATLAS analysis is in disagreement with the data by the FNAL-E-866 experiment on the ratio of the proton and deuteron DY-process cross sections [15], which are commonly used to constrain the sea iso-spin asymmetry $x(\bar{d} - \bar{u})$ in global PDF fits. Indeed, the value of $x(\bar{d} - \bar{u})$ extracted from the FNAL-E-866 data in the Born approximation is positive for the whole range of x and in the ATLAS analysis [14] negative values are preferred. This means, the enhancement of the strange sea observed by ATLAS is obtained at the expense of a suppression of the d -quark PDF. Note, that negative values of $x(\bar{d} - \bar{u})$ were also observed in the NNPDF fit [16] based on collider data only and a corresponding strange sea enhancement appears there, too. Meanwhile, the discrepancy between the ATLAS results and the FNAL-E-866 data is not dramatic and amounts to about 2σ only. Moreover, the ATLAS result on r_s is in agreement with ours within the errors, cf. Fig. 1. On the other hand, the ATLAS data on the W - and Z -boson production [17] are well described by the PDF set with

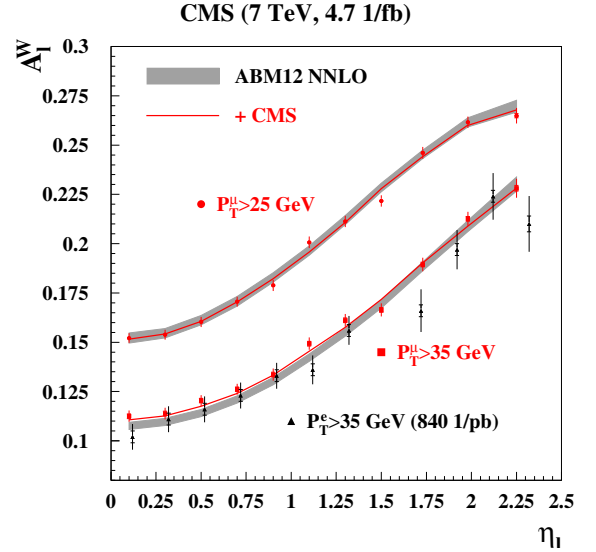


Figure 5: The CMS data on the muon asymmetry [10] with the cuts of $P_T^\mu > 25 \text{ GeV}$ (circles) and $P_T^\mu > 35 \text{ GeV}$ (squares) imposed on the transverse muon momentum in comparison with the NNLO ABM12 prediction error band due to the PDF uncertainties (shaded area) and the earlier CMS data on the electron asymmetry [18] with the cut of $P_T^\mu > 35 \text{ GeV}$ (triangles). The curves display the variant of ABM12 fit [6] with the CMS data of Ref. [10] included.

the suppressed strange sea. In particular, in the updated variant of the ABM12 fit with the NOMAD and CHORUS data included we get a value of $\chi^2 = 35$ for 30 data points in the combined ATLAS W - and Z -data set. In summary, these findings rather point at an insufficient statistical potential of the data used in the ATLAS analysis of Ref. [14] in disentangling the quark PDFs than at a real strange sea enhancement. In this context it is also worth noting that in the analysis of Ref. [10] based on the combination of the CMS and HERA data the strange sea suppression at $x \gtrsim 0.01$ was observed, cf. Fig. 1.

3. Constraints on the non-strange quark PDFs

Recent data on the muon asymmetry A_μ obtained by CMS [10] for the sample with an integrated luminosity of 4.7 1/fb are compared with the predictions based on the NNLO ABM12 PDFs [6] in Fig.5. The predicted central values and their uncertainties due to PDFs are computed with DYNL0 (version 1.3) [19] and FEWZ (version 3.1 [20]), respectively, because the former code shows a better numerical convergence, while the latter allows for a parallel computation with different PDF set members. The agreement between data and the

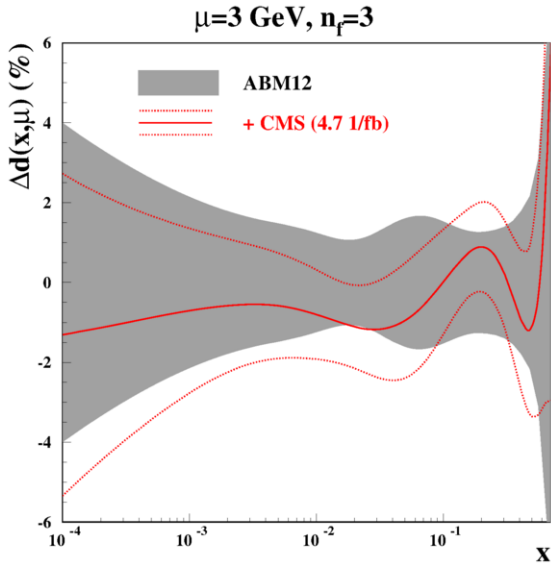


Figure 6: The 1σ fractional error band for the ABM12 d -quark distribution (shaded area) in comparison with the relative variation of its central value due to adding the CMS muon asymmetry data [10] (solid curve). The dotted curves correspond to the d -quark distribution uncertainty in this variant of the ABM12 fit [6].

predictions is in general quite good. For the data sample with $P_T^\mu > 35$ GeV the predictions do somewhat undershoot the data at the muon pseudo-rapidity $\eta_\mu \lesssim 1$ since the ABM12 PDF were tuned to the earlier CMS data on the electron asymmetry [18], which go lower than the muon ones, cf. Fig. 5. However, this tension is within the 1σ PDF uncertainties. Furthermore, for the data sample with $P_T^\mu > 25$ GeV a tension does not show up. Therefore the ABM12 fit does not change significantly due to inclusion of the CMS data on the electron asymmetry. The values of χ^2 obtained in the variants of this fit with the data at $P_T^\mu > 25$ GeV and $P_T^\mu > 35$ GeV included are 16 and 10, respectively, for 11 data points. The former value is somewhat worse than the ideal one due to the data fluctuations at $\eta_\mu \sim 1.5$ going beyond the experimental errors quoted. The change in the ABM12 PDFs due to the CMS muon asymmetry data is within 1σ with the most significant impact observed for the d -quark distribution. The uncertainty in the latter at $x \sim 0.1$ is also somewhat improved, cf. Fig. 6.

In contrast with the CMS muon asymmetry and the related LHC data in general, the Tevatron data on the charged lepton asymmetry do not demonstrate a good agreement with the ABM12 predictions. In particular, recent D0 results on the muon asymmetry [11] obtained with the integral luminosity of 7.3 1/fb signifi-

cantly overshoot the ABM12 predictions at $\eta_\mu \gtrsim 1$, cf. Fig. 7. A discrepancy is especially pronounced for the sample with the cut of $P_T^\mu > 35$ GeV. In this case the shape of the ABM12 predictions differ from the data even qualitatively. The agreement is improved in case the D0 data are added to the ABM12 fit. However, even in this case the profile of data at $P_T^\mu > 35$ GeV is not entirely reproduced and the value of χ^2 is 40 for 10 data points. A better value of $\chi^2 = 14$ can be achieved in a model-independent fit with a 5-th order polynomial. However, in this case the fitted curve exhibits a step at $\eta_\mu \sim 1$, which evidently cannot be provided with a smooth PDF shape. The same step, although less pronounced, appears in the profile of the D0 sample with $P_T^\mu > 25$ GeV, cf. Fig. 7. It is worth noting that the MSTW08 PDFs being tuned to the earlier Tevatron data also demonstrate poor agreement with the D0 data of Ref. [11]. This may point to a disagreement with the earlier Tevatron data. These issues should evidently be clarified before the recent D0 data can be included into our PDF fit.

4. Conclusion

In conclusion, we find that the ABM strange sea distribution can be essentially improved at $x \gtrsim 0.01$ by adding to the fit recent NOMAD and CHORUS data on the charm production in the DIS neutrino-nucleon scattering. The updated PDFs are in agreement with the ABM12 ones although the CHORUS data obtained on the emulsion target demonstrate a particular trend w.r.t. the results of dimuon experiments NuTeV, CCFR, and NOMAD pulling strange sea somewhat up. The CMS and ATLAS data on the associated $(W+c)$ production in the proton-proton collisions, which are also sensitive to the strangeness content of nucleon, overshoot the ABM predictions, however, statistical significance of the discrepancy is inessential in view of the large data uncertainties and foreseen impact of the NNLO corrections to this process. From the variant of the ABM fit based on the CHORUS, CMS, and ATLAS data preferring enhanced strange sea we estimate an upper margin of such enhancement as 20%.

The recent CMS high-statistics data on the muon asymmetry are in a good agreement with the ABM12 NNLO predictions and allow further improvement in disentangling the u - and d -quark distributions. As a result, the uncertainty in ABM d -quark distribution at $x \sim 0.1$ can be reduced by adding the CMS sample to the fit. At the same time, the D0 data on the muon asymmetry, which can potentially further improve the

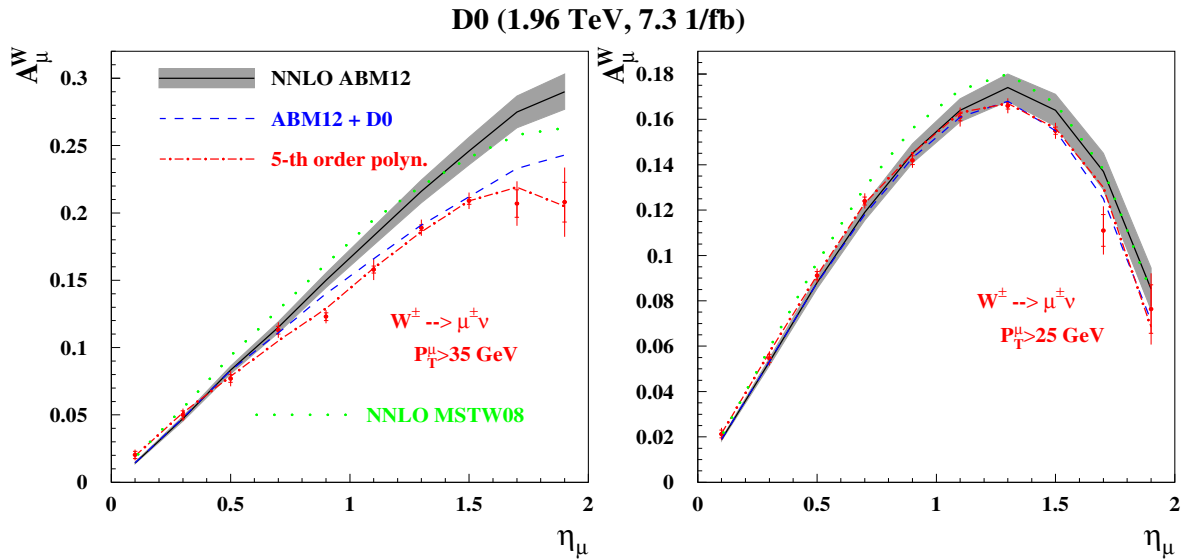


Figure 7: The muon asymmetry data obtained by the D0 collaboration [11] for integral luminosity of 7.3 1/fb with the cuts on the muon transverse momentum $P_T^\mu > 35$ GeV (left panel) and $P_T^\mu > 25$ GeV (right panel) in comparison with the NNLO predictions based on the ABM12 PDFs (solid curves: central values, shaded area: the uncertainties due to PDFs) and the central values for the MSTW08 [21] ones (dots). The variant of the ABM12 fit [6] including the D0 data [11] and the model-independent polynomial fit to the D0 data only are displayed by dashes and dotted-dashes, respectively.

quark PDF uncertainties at bigger values of x , demonstrate poor agreement with the ABM12 predictions and cannot be employed in our analysis before clarification of these discrepancies.

Acknowledgments. We would to thank P. Marquard for careful reading of the text and valuable comments. This work has been supported in part by Helmholtz Gemeinschaft under contract VH-HA-101 (*Alliance Physics at the Terascale*), DFG Sonderforschungsbereich/Transregio 9 and by the European Commission through contract PITN-GA-2010-264564 (*LHCPhenoNet*). We thank the Galileo Galilei Institute for Theoretical Physica for the hospitality and the INFN for partial support during the completion of this work.

References

- [1] M. Goncharov *et al.* [NuTeV Collaboration], Phys. Rev. D **64** (2001) 112006 [hep-ex/0102049].
- [2] O. Samoylov *et al.* [NOMAD Collaboration], Nucl. Phys. B **876** (2013) 339 [arXiv:1308.4750 [hep-ex]].
- [3] A. Kayis-Topaksu, G. Onengut, R. van Dantzig, M. de Jong, R. G. C. Oldeman, M. Guler, U. Kose and P. Tolun *et al.*, New J. Phys. **13** (2011) 093002 [arXiv:1107.0613 [hep-ex]].
- [4] S. Alekhin, S. A. Kulagin and R. Petti, Phys. Lett. B **675** (2009) 433 [arXiv:0812.4448 [hep-ph]].
- [5] S. Alekhin, J. Blümlein and S. Moch, Phys. Rev. D **86** (2012) 054009 [arXiv:1202.2281 [hep-ph]].
- [6] S. Alekhin, J. Blümlein and S. Moch, Phys. Rev. D **89** (2014) 054028 [arXiv:1310.3059 [hep-ph]].
- [7] S. Alekhin, J. Blümlein, L. Caminada, K. Lipka, K. Lohwasser, S. Moch, R. Petti and R. Placakyte, arXiv:1404.6469 [hep-ph].
- [8] S. Chatrchyan *et al.* [CMS Collaboration], JHEP **1402** (2014) 013 [arXiv:1310.1138 [hep-ex]].
- [9] G. Aad *et al.* [ATLAS Collaboration], JHEP **1405** (2014) 068 [arXiv:1402.6263 [hep-ex]].
- [10] S. Chatrchyan *et al.* [CMS Collaboration], arXiv:1312.6283 [hep-ex].
- [11] V. M. Abazov *et al.* [D0 Collaboration], Phys. Rev. D **88** (2013) 091102 [arXiv:1309.2591 [hep-ex]].
- [12] N. Ushida *et al.* [Fermilab E531 Collaboration], Phys. Lett. B **206** (1988) 375.
- [13] A. Kayis-Topaksu *et al.* [CHORUS Collaboration], Phys. Lett. B **626** (2005) 24.
- [14] G. Aad *et al.* [ATLAS Collaboration], Phys. Rev. Lett. **109** (2012) 012001 [arXiv:1203.4051 [hep-ex]].
- [15] R. S. Towell *et al.* [NuSea Collaboration], Phys. Rev. D **64** (2001) 052002 [hep-ex/0103030].
- [16] R. D. Ball, V. Bertone, S. Carrazza, C. S. Deans, L. Del Debbio, S. Forte, A. Guffanti and N. P. Hartland *et al.*, Nucl. Phys. B **867** (2013) 244 [arXiv:1207.1303 [hep-ph]].
- [17] G. Aad *et al.* [ATLAS Collaboration], Phys. Rev. D **85** (2012) 072004 [arXiv:1109.5141 [hep-ex]].
- [18] S. Chatrchyan *et al.* [CMS Collaboration], Phys. Rev. Lett. **109** (2012) 111806 [arXiv:1206.2598 [hep-ex]].
- [19] S. Catani, L. Cieri, G. Ferrera, D. de Florian, M. Grazzini, Phys. Rev. Lett. **103**, 082001 (2009), arXiv:0903.2120.
- [20] Y. Li and F. Petriello, Phys. Rev. D **86**, 094034 (2012), arXiv:1208.5967.
- [21] A. Martin, W. Stirling, R. Thorne, and G. Watt, Eur. Phys. J. C **63**, 189 (2009), arXiv:0901.0002.